Inorganic Chemistry

Article

pubs.acs.org/IC

Molybdenum(VI) Coordination Chemistry of the N,N-Disubstituted Bis(hydroxylamido)-1,3,5-triazine Ligand, H_2bihyat. Water-Assisted Activation of the Mo^{VI}=O Bond and Reversible Dimerization of *cis*-[$Mo^{VI}O_2$(bihyat)] to [$Mo^{VI}_2O_4$(bihyat)$_2$(H_2O)$_2$]

Marios Stylianou,[†] Vladimiros A. Nikolakis,[‡] George I. Chilas,[‡] Tamas Jakusch,[§] Tiverios Vaimakis,*[,‡] Tamas Kiss,*[,§] Michael P. Sigalas,*[,⊥] Anastasios D. Keramidas,*[,†] and Themistoklis A. Kabanos*[,‡]

[†]Department of Chemistry, University of Cyprus, Nicosia 1678, Cyprus

[‡]Section of Inorganic and Analytical Chemistry, Department of Chemistry, University of Ioannina, Ioannina 45110, Greece

[§]Department of Inorganic and Analytical Chemistry, University of Szeged, Szeged, Hungary

[⊥]Laboratory of Applied Quantum Chemistry, Department of Chemistry, Aristotle University of Thessaloniki, Thessaloniki 54124, Greece

Supporting Information

ABSTRACT: Reaction of the N,N-disubstituted bis(hydroxylamino) ligand 2,6-bis[hydroxy(methyl)amino]-4-morpholino-1,3,5-triazine (H_2bihyat) with *cis*-[$Mo^{VI}O_2$(acac)$_2$] in tetrahydrofuran resulted in isolation of the mononuclear compound *cis*-[$Mo^{VI}O_2$(bihyat)] (**1**). The treatment of $Na_2Mo^{VI}O_4{\cdot}2H_2O$ with the ligand H_2bihyat in aqueous solution gave the dinuclear compounds *cis*-[$Mo^{VI}_2O_4$(bihyat)$_2$(H_2O)$_2$] (**2**) and *trans*-[$Mo^{VI}_2O_4$(bihyat)$_2$(H_2O)$_2$] (**3**) at pH values of 3.5 and 5.5, respectively. The structures for the three molybdenum(VI) compounds were determined by X-ray crystallography. Compound **1** has a square-pyramidal arrangement around molybdenum, while in the two dinuclear compounds, each molybdenum atom is in a distorted pentagonal-bipyramidal environment of two bridging and one terminal oxido groups, a tridentate (O,N,O) bihyat^{2-} ligand that forms two five-membered chelate rings, and a water molecule trans to the terminal oxido group. The dinuclear compounds constitute rare examples containing the {$Mo_2^{VI}O_2(\mu_2\text{-}O_2)$}$^{4+}$ moiety. The potentiometry revealed that the Mo^{VI}bihyat^{2-} species exhibit high hydrolytic stability in aqueous solution at a narrow range of pH values, 3−5. A subtle change in the coordination environment of the five-coordinate compound **1** with ligation of a weakly bound water molecule trans to the oxido ligand (**1w**) renders the equatorial oxido group in **1w** more nucleophilic than that in **1**, and this oxido group attacks a molybdenum atom and thus the dinuclear compounds **2** and **3** are formed. This process might be considered as the first step of the oxido group nucleophilic attack on organic substrates, resulting in oxidation of the substrate, in the active site of molybdenum enzymes such as xanthine oxidase. Theoretical calculations in the gas phase were performed to examine the influence of water on the dimerization process (**1** → **2**/**3**). In addition, the molecular structures, cis/trans geometrical isomerism for the dinuclear molybdenum(VI) species, vibrational spectra, and energetics of the metal−ligand interaction for the three molybdenum(VI) compounds **1**−**3** have been studied by means of density functional theory calculations.

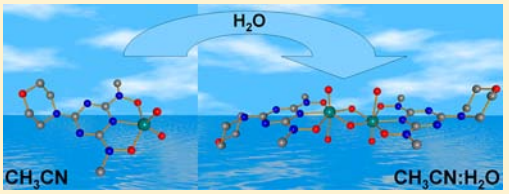

INTRODUCTION

Molybdenum enzymes are present in all forms of life, ranging from ancient bacteria to humans, and, with the exception of the nitrogenases,[1,2] mostly catalyze oxido-transfer reactions.[3,4] Molybdenum-catalyzed epoxidation is also an important process for the production of both bulk and fine chemicals: it remains the basis for the industrial production of propylene oxide and is a convenient laboratory method for epoxidation of more complicated alkyl olefins.[5,6]

The concentration of molybdate, [$Mo^{VI}O_4$]$^{2-}$, in seawater, ca. 100 nM,[7] makes molybdenum the most abundant transition metal in seawater, which presumably means that biological systems take molybdenum from the sea. Thus, it is of vital importance to further explore the aqueous chemistry of molybdenum(VI). Hydroxylamine ligands play an important role in the sequestration of hard metal ions in biological systems. For example, the naturally occurring hydroxylamine ligand *N*-hydroxy-*α*,*α*-iminodipropionate (hidpa^{3-}) is utilized from mushrooms (of genus Amanita[8]) as a selective chelator for vanadium,[9] forming a thermodynamically and hydrolytically[10] quite stable vanadium complex, [V(hidpa)$_2$]$^{2-}$ (Scheme 1). Its molybdenum analogue,[11] [Mo(hidpa)$_2$]$^-$ (Scheme 1), possesses also great thermodynamic and hydrolytic stability.

Recently, Melman and co-workers[12] reported a new family of compact pincer tridentate chelators, based on an N,N-

Received: June 18, 2012
Published: December 5, 2012

   dx.doi.org/10.1021/ic301282q | Inorg. Chem. 2012, 51, 13138−13147

Scheme 1

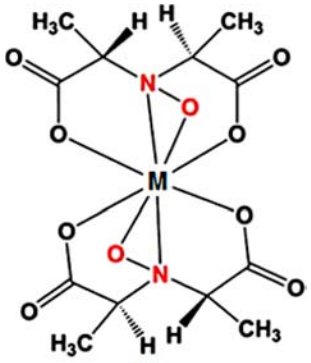

disubstituted bis(hydroxyamino)-1,3,5-triazine motif (H_2bht, Scheme 2), that possesses high affinity and hydrolytic stability

Scheme 2

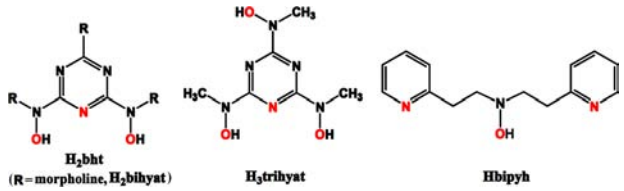

for iron(III) and titanium(IV). Moreover, our group reported that this family of N,N-disubstituted bis/tris(hydroxylamino)-1,3,5-triazine ligands (H_2bihyat and H_3trihyat; Scheme 2) possesses also high affinity and hydrolytic stability for vanadium(V)[13] over a wide pH range of 3−11.

Although the coordination chemistry of unmodified hydroxylamine and its alkyl-substituted derivatives with molybdenum[14] and vanadium[15] was extensively studied, the ligation of molybdenum and vanadium[13,16] with chelating hydroxylamino (chehyl) ligands remains surprisingly unexplored.

A literature survey revealed that the metal-binding properties of only three chelating N,N-disubstituted hydroxylamino ligands, except for H_3hidpa, have been very recently reported[12,13,17] (Scheme 2). On the basis of these facts and taking into account the thermodynamic and hydrolytic stability of vanadium(V) with the ligands H_2bihyat[13a] and H_3trihyat[13b] (Scheme 2), we embarked on an effort to prepare molybdenum(VI) compounds with the chehyl ligand 2,6-bis[hydroxy(methyl)amino]-4-morpholino-1,3,5-triazine (H_2bihyat) shown in Scheme 2.

In the present study, the synthesis and structural and physicochemical characterization of the mononuclear compound *cis*-[$Mo^{VI}O_2$(bihyat)] (**1**) and of the dinuclear species *cis/trans*-[$Mo^{VI}_2O_2(\mu_2\text{-}O_2)$(bihyat)$_2(H_2O)_2$] (**2/3**) are reported. The potentiometry shows that the Mo^{VI}bihyat^{2-} species exhibit high hydrolytic stability in aqueous solution at a narrow range of pH values, 3−5. The distinctive structural features of the N,N-disubstituted hydroxylamido ligand bihyat^{2-}, including the rigid planar geometry and the strong binding properties of the hard donor atoms, activate the Mo^{VI}═O group in the presence of water, resulting in dimerization of **1** to **2/3**. In addition, density functional theory calculations have been carried out for the mononuclear and dinuclear molybdenum(VI) compounds in order to examine their geometrical isomerism, the nature and relative strength of the metal−ligand interaction, and the energetics of the dimerization process (**1** → **2/3**) and to elucidate their vibrational spectra.

EXPERIMENTAL SECTION

Materials. Mo^VCl_5 and *N*-methylhydroxylamine hydrochloride were purchased from Merck and Fluka, respectively, and $Na_2Mo^{VI}O_4\cdot 2H_2O$, *cis*-[$Mo^{VI}O_2$(acac)$_2$], morpholine, and 2,4,6-trichloro-1,3,5-triazine from Aldrich and used without any further purification. C, H, and N analyses were conducted by the microanalytical service of the Department of Chemistry, University of Hamburg. Molybdenum was determined by atomic absorption. The ligand H_2bihyat was prepared by a literature procedure[12c] and recrystallized from isopropyl alcohol. Its purity was confirmed by elemental analysis (C, H, and N), IR spectroscopy, melting point, and ^{1}H and ^{13}C NMR spectroscopy.

{2,6-Bis[hydroxy(methyl)amino]-4-morpholino-1,3,5-triazinato-*O*,*N*,*O*}-*cis*-dioxidomolybdenum(VI) (1; *cis*-[$Mo^{VI}O_2$(bihyat)]). *cis*-[$Mo^{VI}O_2$(acac)$_2$] (0.250 g, 0.770 mmol) was dissolved in anhydrous tetrahydrofuran (10 mL) at ambient temperature (27 °C) with magnetic stirring. Then, solid H_2bihyat (0.196 g, 0.770 mmol) was added in one portion to the above stirred solution. Upon addition of the ligand, the colorless solution turned yellow. After 5 h of stirring, the solution was filtered, to the filtrate was added hexane (30 mL), and the stirring was continued for an additional 10 min. The resulting yellow precipitate was collected on a glass frit and washed two times with 10 mL of hexane. The solid was dried in vacuo and yielded 0.20 g (68%) of a light-yellow powder identified as **1**. Elem anal. Calcd for $C_9H_{14}N_6O_5Mo$ (382.20): C, 28.26; H, 3.69; N, 21.99; Mo, 25.10. Found: C, 28.24; H, 3.69; N, 21.78; Mo, 25.13. ^{1}H NMR ($CDCl_3$): δ 3.49 (6H, s), 3.77 (3H, t), 3.92 (3H, t). ^{13}C NMR ($CDCl_3$): δ 36.27 ($C_{4,5}$), 44.82 ($C_{6,8}$), 66.61 ($C_{7,9}$).

Single crystals of **1** suitable for X-ray structure analysis were grown by layering hexane into a concentrated tetrahydrofuran solution of the compound.

Bis(μ_2-oxido)bis{2,6-bis[hydroxy(methyl)amino]-4-morpholino-1,3,5-triazinato-*O*,*N*,*O*}bis[*cis*-aqua-*cis*-oxidomolybdenum(VI)] (2·0.4H_2O; *cis*-[$Mo_2^{VI}O_2(\mu_2\text{-}O_2)$(bihyat)$_2(H_2O)_2$]·0.4$H_2O$). $Na_2Mo^{VI}O_4\cdot 2H_2O$ (0.150 g, 0.620 mmol) was dissolved in water (8 mL) under magnetic stirring at ambient temperature (25 °C). The alkaline pH of the solution (∼8.5) was adjusted to ∼3.5 with an aqueous hydrochloric acid solution (2 M) and then solid H_2bihyat (0.154 g, 0.600 mmol) was added in one portion to the above stirred solution. Upon addition of the ligand, the colorless solution turned orange, and an orange precipitate formed. The pH of the reaction mixture was kept at pH ∼3.5 with 2 M HCl. After an additional 12 h of stirring, the precipitate was filtered off, washed with 4.0 mL of water and then with 5 mL of methyl alcohol, and dried in vacuo. Yield: 0.14 g (58% based on H_2bihyat). Elem anal. Calcd for $C_{18}H_{32.8}N_{12}O_{12.4}Mo_2$ (807.43): C, 26.75; H, 4.09; N, 20.82; Mo, 23.76. Found: C, 26.70; H, 4.19; N, 20.72; Mo, 23.70. ^{1}H NMR (D_2O, 0.10 M KCl, pD 3.4, 2.00 mM): δ 3.54 (6H, s), 3.79 (3H, t), 3.89 (3H, t). ^{13}C NMR (D_2O, 0.10 M KCl, pD 3.4, 2.00 mM): δ 35.96 ($C_{4,5}$), 44.36 ($C_{6,8}$), 66.29 ($C_{7,9}$). Single crystals of 2·8D_2O suitable for X-ray structure analysis were grown as described in the experimental section of the Supporting Information (SI).

Bis(μ_2-oxido)bis{2,6-bis[hydroxy(methyl)amino]-4-morpholino-1,3,5-triazinato-*O*,*N*,*O*}-bis[*trans*-aqua-*trans*-oxidomolybdenum(VI)] (3·1.7H_2O; *trans*-[$Mo_2^{VI}O_2(\mu_2\text{-}O_2)$(bihyat)$_2(H_2O)_2$]·1.7$H_2O$). This compound was synthesized in an manner analogous to that of compound 2·0.4H_2O except that the final pH[18] of the solution was 5.5 in 73% yield. Elem anal. Calcd for $C_{18}H_{35.4}N_{12}O_{13.7}Mo_2$ (830.85): C, 26.00; H, 4.29; N, 20.23; Mo, 23.09. Found: C, 26.05; H, 4.29; N, 20.32; Mo, 23.00. ^{1}H NMR (D_2O, 0.10 M KCl, pD 5.3, 2.00 mM): δ 3.55 (6H, s), 3.79 (3H, t), 3.92 (3H, t). ^{13}C NMR was not observed because of the low concentration of the complex. Single crystals of 3·2D_2O·2CD_3CN suitable for X-ray

dx.doi.org/10.1021/ic301282q | Inorg. Chem. 2012, 51, 13138−13147

Scheme 3

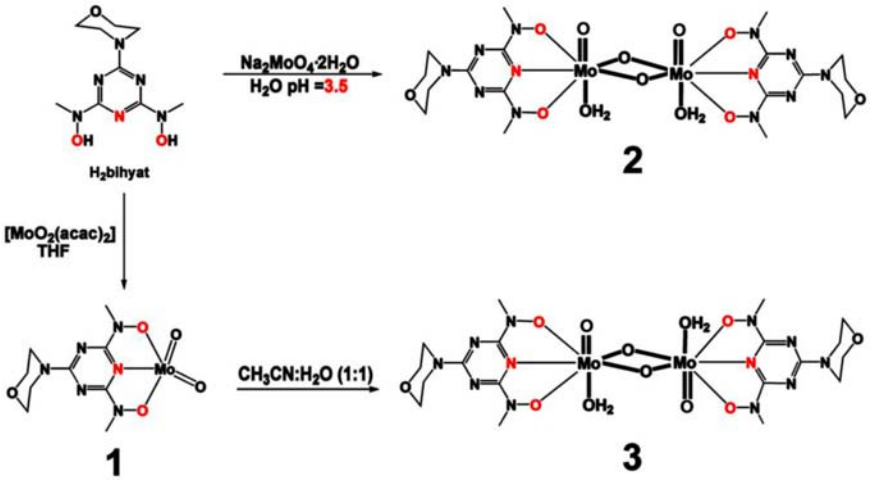

structure analysis were grown as described in the experimental section of the Supporting Information.

The IR spectra of complexes **2** and **3** in KBr are shown in Figure S1 in the Supporting Information.

RESULTS AND DISCUSSION

Synthesis. Compounds **1** (mononuclear), **2** (cis dinuclear), and **3** (trans dinuclear) were synthesized according to Scheme 3. The mononuclear complex **1** was prepared by the treatment of *cis*-$[Mo^{VI}O_2(acac)_2]$ (eq 1) with an equivalent quantity of the ligand H_2bihyat.

$$cis\text{-}[Mo^{VI}O_2(acac)_2] + H_2bihyat \rightarrow cis\text{-}[Mo^{VI}O_2(bihyat)] + 2Hacac \quad (1)$$

The dinuclear species **2** and **3** were prepared by reacting $Na_2Mo^{VI}O_4\cdot 2H_2O$ with H_2bihyat in water (eq 2) at pH values of 3.5 and 5.5,[18] respectively. Solvation and hydrogen bonding presumably stabilize the more polar cis isomer than the trans isomer at lower pH values.

$$2Na_2Mo^{VI}O_4\cdot 2H_2O + 2H_2bihyat \rightarrow cis/trans\text{-}[Mo^{VI}{}_2O_2(\mu_2\text{-}O)_2(bihyat)_2(H_2O)_2] + 4NaOH + 2H_2O \quad (2)$$

Efforts to isolate the molybdenum(V) species with the ligand H_2bihyat using Mo^VCl_5 as the source of molybdenum(V) and water as the solvent were unsuccessful because we always ended up with the dinuclear molybdenum(VI) compound **2** (eq 3).[19] This is something expected on the basis of the interaction of vanadium with H_2bihyat, in which vanadium(V) compounds were always isolated irrespective of the vanadium(IV) source and the conditions used.[13a,16]

$$2Mo^VCl_5 + \frac{1}{2}O_2 + 2H_2bihyat + 5H_2O \rightarrow cis\text{-}[Mo^{VI}{}_2O_2(\mu_2\text{-}O)_2(bihyat)_2(H_2O)_2] + 10HCl \quad pH\ 3.5 \quad (3)$$

The mononuclear compound **1** is soluble in nonpolar solvents such as acetonitrile, tetrahydrofuran, chloroform, dichloromethane, etc., while the dinuclear compounds are very slightly soluble.

Crystal Structures. A summary of the crystallographic data and final refinement details for compounds **1**–**3** are given in Table S1 in the SI. The molecular structure of compound **1** is shown in Figure 1. A selection of interatomic distances and

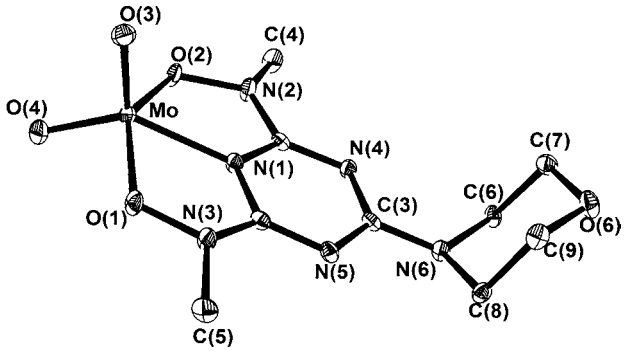

Figure 1. ORTEP representation of compound **1** at 50% probability ellipsoids with atomic numbering.

bond angles relevant to the molybdenum coordination sphere in **1** is listed in Table S2 in the SI. The molybdenum atom has an almost ideal square-pyramidal geometry ($\tau = 0.104$)[20] and is bonded to a tridentate bihyat^{2-} ligand at the triazine nitrogen atom [d(Mo−N_{tr}) = 2.063(2) Å] and the two deprotonated hydroxyamido oxygen atoms [d(Mo−O_h) ∼ 1.99 Å] as well as two oxido groups [O(3) and O(4)].

The molecular structures of the dinuclear compounds **2** and **3** are shown in Figures 2 and 3, respectively. A selection of interatomic distances and bond angles relevant to the molybdenum coordination sphere in **2** and **3** is listed in Tables S3 and S4 in the SI, respectively. In compounds **2** and **3**, each molybdenum atom is in a distorted pentagonal-bipyramidal environment of two bridging and one terminal oxido groups, a tridentate (O,N,O) bihyat^{2-} ligand that forms two five-membered chelate rings, and a water molecule trans to the terminal oxido group. Compounds **2** and **3** appear to be rare[14a,21] examples containing the $\{Mo^{VI}{}_2O_4\}^{4+}$ moiety. Interestingly, the two terminal oxygen atoms [O(3) and O(13)] in **2** are in the cis position relative to each other, which is in contrast to the trans arrangement observed for this class[14a,21] of $\{Mo^{VI}{}_2O_4\}^{4+}$ compounds. In the chemistry of the molybdenum(V) species, the $\{Mo^V{}_2O_4\}^{2+}$ moiety is quite

dx.doi.org/10.1021/ic301282q | Inorg. Chem. 2012, 51, 13138−13147

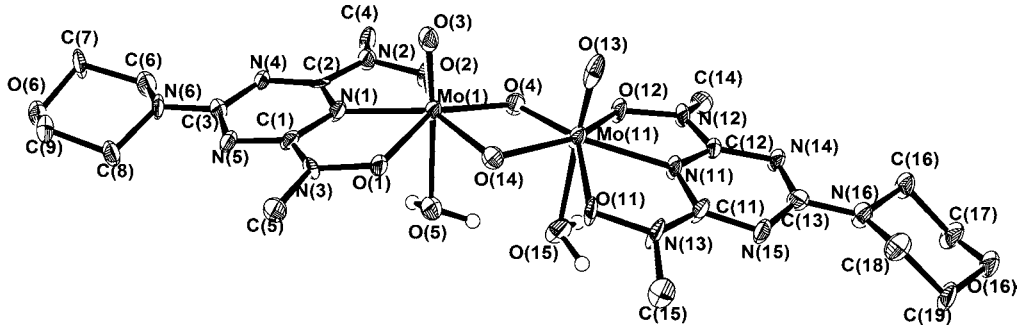

Figure 2. ORTEP representation of compound **2** at 50% probability ellipsoids with atomic numbering.

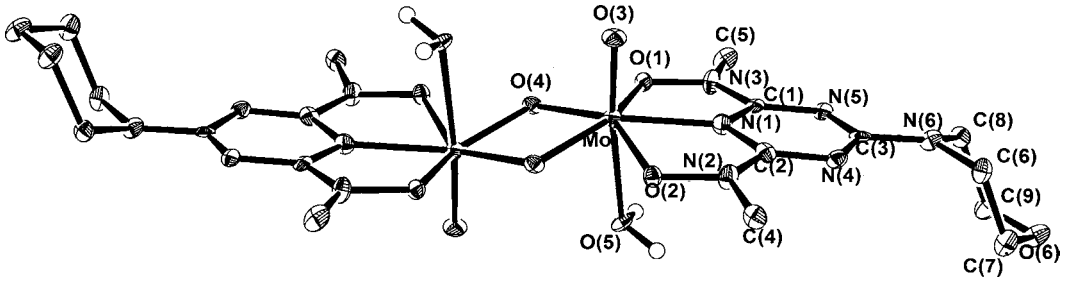

Figure 3. ORTEP representation of the anion of compound **3** at 50% probability ellipsoids with atomic numbering.

common, and the terminal oxido groups are found to be nearly exclusively in the cis position.[22]

NMR Spectroscopy. The ^{13}C NMR data deduced from 2D $\{^{1}H,^{13}C\}$ gz-HQSC NMR spectra (Figure S2 in the SI) of the ligand H_2bihyat (see Scheme 4 for atom numbering) and of the molybdenum(VI) compounds in various solvents and their complexation-induced shifts (cis) are shown in Table 1. The $\Delta_{cis}(C_{4,5})$ [$\Delta_{cis} = \delta_{complex} - \delta_{ligand}$] values are in the range −0.72 to −1.43 ppm, and this means that the ligand(s) remain(s) bonded to the molybdenum(VI) atom at the triazine nitrogen atom and the two deprotonated hydroxyamido oxygen atoms. The mononuclear compound **1** in CD_3CN and $CDCl_3$ has moderate deshielding for $C_{4,5}$ (∼−0.8 ppm), while in D_2O, the large deshielding of −1.43 ppm for $C_{4,5}$ induced by ligation of bihyat^{2-} to the molybdenum(VI) atom has been assigned to the dinuclear species that are formed in D_2O, as was evidenced by potentiometry, ^1H NMR, and UV−vis spectroscopies (vide infra) and from the isolation and crystallographic characterization of the dinuclear compounds **2** and **3** from D_2O (pD 3.8) and from mixtures of CD_3CN and D_2O, respectively.

Scheme 4

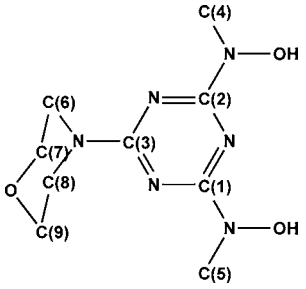

The ^1H NMR spectra of the monomer, i.e., compound **1**, in CD_3CN and dimer (in D_2O, pD 3.5) also gave different chemical shifts for $H_3C(4,5)$ ($\delta_{monomer} - \delta_{dimer}$ = 0.18 ppm); however, the larger differences were observed for the remote protons from the metal center, $H_2C(7,9)$ ($\delta_{monomer} - \delta_{dimer}$ = 0.80 ppm). The $H_3C(4,5)$ groups are close to the molybdenum atom, and variation of the chemical shifts of the attached protons is expected because of the different coordination environments of the metal center between the monomer and dimers. However, deshielding of the distant protons from the metal center, $H_2C(7,9)$, observed for the monomer is unexpected. In order to explore the origin of these shifts, the crystal structures of the three molybdenum(VI) compounds were examined in great detail. The morpholine rings in the crystal structures of compounds **1** (monomer) and **3** (trans dinuclear) are almost perpendicular to the plane defined by the triazine ring (see Figures 1 and 3, respectively), and thus the

Table 1. ^{13}C NMR Chemical Shifts (ppm) from gHSQC of the Ligand H_2bihyat and of the Molybdenum(VI) Species in Various Solvents

		δ_{ligand} ($\delta_{complex}$)			
solvent	compound	$C_{4,5}$[a]	$C_{6,8}$[a]	$C_{7,9}$[a]	$\Delta_{cis}(C_{4,5})$[b]
$CDCl_3$	**1**	37.11 (36.27)	43.70 (44.82)	66.73 (66.61)	−0.84
CD_3CN	**1**	36.78 (36.06)	44.66 (43.75)	66.13 (66.18)	−0.72
D_2O	*c*	37.39 (35.96)	44.36 (44.36)	66.21 (66.29)	−1.43

[a]Atom numbering as in Scheme 4. [b]$\Delta_{cis} = \delta_{complex} - \delta_{ligand}$. [c]The sample was prepared by mixing equal volumes of 2.00 mM $Na_2Mo^{VI}O_4{\cdot}2H_2O$ and 2.00 mM H_2bihyat in D_2O and 0.10 M KCl, and the pD was adjusted to 3.4 with a DCl solution (0.01 M) in D_2O.

dx.doi.org/10.1021/ic301282q | *Inorg. Chem.* 2012, 51, 13138−13147

carbon atoms C(7) and C(9) are close to the triazine ring {d[C(3)−C(7,9)] = 3.298(4) Å for **1** and ∼3.41 Å for **3**}, while the morpholine ring in **2** (cis dinuclear) lies almost at the same plane with the triazine ring (see Figure 2) with d[C(3)−C(7,9)] = ∼3.65 Å. As a result, the protons attached to carbons C(7) and C(9) in **1** and **3** are exposed to deshielding of the anisotropic magnetic field of the aromatic ring, while in **2**, the corresponding protons are away from the aromatic ring. The different positions of the morpholine ring in **1**−**3** are attributed to deviation of the morpholine nitrogen atom from the plane defined by the carbon atoms C(3), C(6), and C(8) (Scheme 4). The four atoms C(3), C(6), C(8), and N_m] (Scheme 4) are almost homoplanar, showing an sp^2 hybridization for the morpholine nitrogen atom[12c] (resonance form B, Scheme 5).

Scheme 5

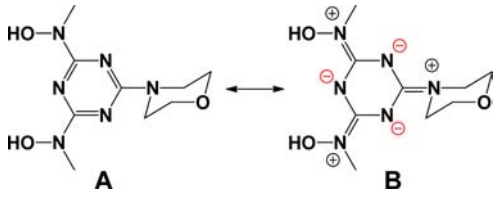

However, the morpholine nitrogen atom deviates slightly above the plane defined by the three carbon atoms in the structure of **2** [0.116(8) Å] and below this plane in the structures of **1** [0.205(3) Å] and **3** [0.132(4) Å]. Thus, the ligand is described as a hybrid of the two resonance forms shown in Scheme 5. The percentage of each resonance form (Scheme 5), and thus the electron-donating strength of the morpholine nitrogen atom to the triazine ring, is dependent on the complex and metal-ion coordination.

To further confirm these assignments, the ^{1}H NMR spectra of **1** in the mixed-solvent system CD_3CN/D_2O (Figure 4) were measured, starting with neat CD_3CN and adding various volumes of D_2O. The addition of even a few drops of D_2O into the CD_3CN solution of **1** resulted in a color change from pale-yellow to brown-red, concomitant with the appearance of a peak at 404 nm (Figure 5) in the UV−vis spectrum of this

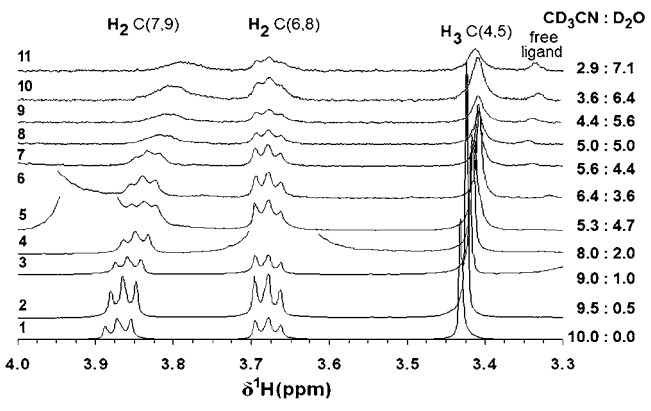

Figure 4. ^{1}H NMR spectra (500 MHz) of **1** in CD_3CN (spectrum 1) and in the mixed-solvent system (CD_3CN/D_2O, v/v). The initial concentration of **1** in CD_3CN was 1.5 mM. Hydrolysis of the molybdenum(VI) compounds and formation of the free ligand H_2bihyat are observed in the CD_3CN/D_2O solutions containing $D_2O \geq 50\%$ v/v (spectra 8−11). The large peaks of spectra 4−6 are due to free H_2O in D_2O. The H_2O peak shifts to lower field as the quantity of D_2O in the solvent system increases.

solution. The peak at 404 nm is characteristic of the dinuclear molybdenum(VI) species (see Figure S3 in the SI).

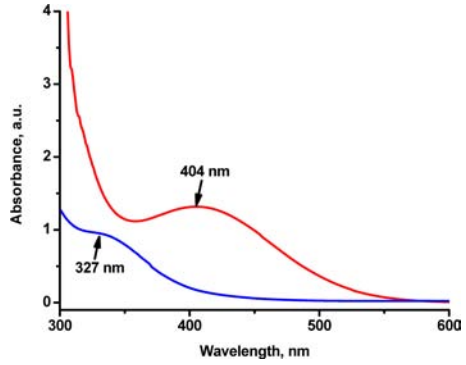

Figure 5. Visible spectra of compound **1** in acetonitrile before (blue line) and after (red line) the addition of water.

In addition, the ^{1}H NMR peak of the $H_3C(4)$ and $H_3C(5)$ protons and the peaks of the protons attached to carbons C(7) and C(9) shift gradually to higher field, indicating formation of the cis/trans dinuclear species. The fact that the addition of water into an acetonitrile solution of **1** shifts the ^{1}H NMR peaks without the appearance of new peaks for the different Mo^{VI}bihyat^{2-} species has been attributed to the very fast interconversion between the molybdenum species, faster than the NMR time scale.

Electrochemistry. The cyclic voltammetric examination of the ligand H_2bihyat and of the mononuclear compound **1** in CH_3CN (Figure S4 in the SI) shows oxidation and reduction waves assigned to the redox activity of the ligand. The peaks of the voltamogram of **1** in CH_3CN are shifted to lower potentials compared to the free ligand because of its ligation to the molybdenum atom. Similarly, the cyclic voltammogram of compound **2** (Figure S5A in the SI) in water (pH 3.52) was very similar to that of the free ligand (Figure S5B in the SI) at the same conditions.

$Mo^{VI}H_2$bihyat Equilibrium Studies. The stability constants of the mononuclear and dinuclear molybdenum(VI) species are summarized in Table 2. The pH dependence of the ^{1}H NMR spectra of the $Mo^{VI}H_2$bihyat system over the pH range of 2−6 (Figure S6 in the SI) reveals that the Mo^{VI}bihyat^{2-} species exhibit the highest stability at pH ∼4. It is evident from the pH dependence of the fraction of the Mo^{VI}bihyat^{2-} species, on the basis of the ^{1}H NMR peak areas (Figure 6), that the dinuclear species are formed. Formation of the dinuclear species was also verified by UV−vis measurements (Figure S7 in the SI). The Mo^{VI}bihyat^{2-} species have absorption maxima at 406 nm (Figure S3 in the SI), while neither the oxidomolybdenum(VI) anions nor the ligand has color in the visible range.

The fitting graphs (Figures 6 and S7 in the SI) and parameters (Table 2) of the data evaluation of all three methods support formation of the dinuclear species. The assumption of the coexistence of both the mononuclear and dinuclear species gives the best result; however, the difference compared to the only dinuclear species model is not significant. The three applied methods give only an estimation of the dimer−monomer equilibrium (log $K_{dimer/monomer}$ = 3.9 ± 0.6), indicating the dominance of the dinuclear species. The speciation curves (Figures 7 and S8 and S9 in the SI) with the assumption of the presence of only the dimer) reveal that

dx.doi.org/10.1021/ic301282q | Inorg. Chem. 2012, 51, 13138−13147

Table 2. Formation Constants (log β) for the System $H^+Mo^{VI}O_4^{2-}$Hbihyat^{-a} (HL^-)

	log β_{311} [$MoO_2(L)$]	fitting parameter	log β_{311}/logβ_{622} [log$K$] [$MoO_2(L)$]/ [$(MoO_2(L)_2$]	fitting parameter	log β_{622} [$(MoO_2(L)_2$]	fitting parameter
pH metry	21.12(2)	1.8×10^{-3} [b]	20.94(19)/45.10(36) [3.22]	1.7×10^{-3} [b]	*45.61(3)*	1.9×10^{-3} [b]
^{1}H NMR	21.26(3)	3.7×10^{-2} [c]	20.64(28)/45.63(9) [4.35]	2.0×10^{-2} [c]	*45.75(2)*	2.1×10^{-2} [c]
UV–vis	21.51(1)	1.6×10^{-2} [d]	20.99(4)/45.97(9) [4.05]	4.0×10^{-3} [d]	*46.15(1)*	6.4×10^{-3} [d]
average			**20.85(20)/45.6(4)** [3,9(6)]		*45.84(28)*	

[a]Because an accurate pK_a value of Hbihyat$^-$ could not be determined by potentiometry (the deprotonation of Hbihyat$^-$ could not be detected until pH 11.7, I = 0.20 KCl, 25.0 °C),[13a] it has been assumed that Hbihyat$^-$ cannot be deprotonated to bihyat^{2-}. [b]The average difference between the calculated and experimental titration curves expressed in cm^3 of the titrant. [c]The average difference between the fitted and directly calculated mole fractions. [d]The average difference between the calculated and experimental absorbance values.

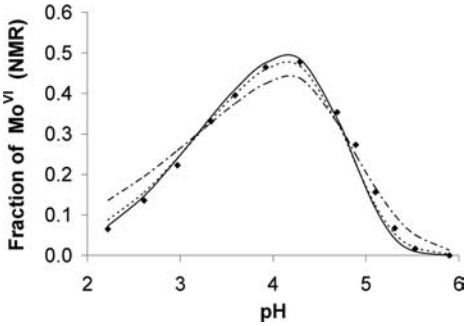

Figure 6. Fraction of the detected Mo^{VI}bihyat^{2-} species over the pH range of 2–6, calculated from integration of the ^{1}H NMR peaks of the free and ligated bihyat^{2-} ligand [$C_{molybdenum}$ = 1.00 mM, $C_{H_2bihyat}$ = 1.00 mM, I = 0.20 M (KCl), and T = 25.0 °C]. The individual points (◆) are calculated from integration of the ^{1}H NMR peaks. The solid line represents the fitted values on the basis of stability constants in the presence of only the dimer [MoO_2(bihyat)]$_2$, the dash-dotted line (–·–) represents the presence of only the monomer *cis*-[MoO_2(bihyat)], and the dotted line (- - -) represents both species.

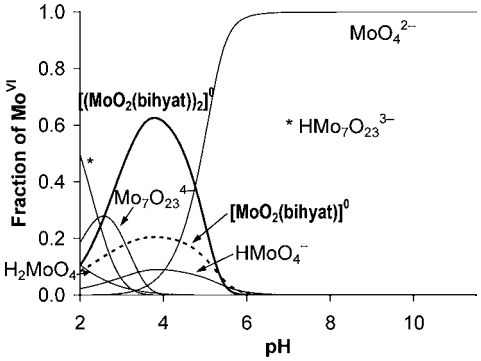

Figure 7. Speciation curves of the molybdenum(VI) species formed in the Mo^{VI}H$_2$bihyat system at a 1:2 metal-to-ligand ratio. $C_{molybdenum(VI)}$ = 0.0010 M, I = 0.20 M, and T = 25.0 °C.

molybdenum(VI) does form stable complexes with bihyat^{2-} over only a narrow pH range (pH 3–5), which is in marked contrast to the high stability of the vanadium(V) species with bihyat^{2-} over a wide pH range in water (pH 3.3–11).[13a]

Thermogravimetric Analysis (TGA). Figure 8 shows the TGA curves for compounds **1** (monomer), **2**·0.4H_2O (cis dimer), and **3**·1.7H_2O (trans dimer), respectively. The thermal decomposition of compound **1** (Figure 8, blue curve) occurs in two exothermic steps (Figure S10 in the SI, blue curve) with an overall weight loss of 62.48%, which corresponds to the removal of an organic ligand, resulting in the formation of molybdenum(VI) oxide, Mo$^{VI}O_3$ (theoretical mass loss 62.34%). The first step is very sharp, takes place at ~185–

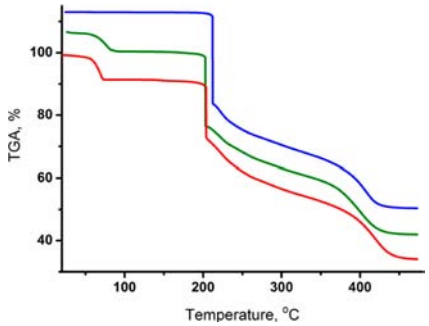

Figure 8. TGA curves of compounds **1** (monomer, blue curve), **2**·0.4H_2O (cis dimer, green curve), and **3**·1.7H_2O (trans dimer, red curve).

215 °C (Figure 8, blue curve), and corresponds to the removal of about half of the ligand. The removal of the remaining part of the ligand takes place up to ~470 °C in the next step. Thermal decomposition of compounds **2**·0.4H_2O and **3**·1.7H_2O has an additional step at ~40–100 °C, which is endothermic (Figures 8 and S10 in the SI, green and red curves, respectively), and it is attributed to the removal of water (ligated and crystalline). After the removal of water, the dinuclear compounds **2**·0.4H_2O and **3**·1.7H_2O exhibit the same thermal behavior (Figure 8) as compound **1** (monomer), which indicates that the dinuclear compounds **2**·0.4H_2O and **3**·1.7H_2O first are converted to the monomer (**1**) and then are decomposed. In order to prove this hypothesis, compound **2**·0.4H_2O was elaborated by a new heating program consisting of two steps, the dynamic step, from ambient temperature (~20 °C) to 90 °C, with a heating rate of β = 2 °C/min, and the isothermal step (1 h) at 90 °C. The light-yellow powder produced (eq 4) is identified as **1** by IR, elemental analysis, and NMR. The weight losses of the additional step are 5.92% for **2**·0.4H_2O and 7.90% for **3**·1.7H_2O, which correspond to the removal of 2.4 and 3.7 water molecules, respectively.

$$\mathbf{2}\cdot 0.4H_2O\ (\text{dimer}) \underset{H_2O}{\overset{90\ ^\circ C}{\rightleftharpoons}} \mathbf{1}\ (\text{monomer}) \qquad (4)$$

THEORETICAL STUDY

Molecular Structures of Compounds 1–3. The optimized molecular structures of compounds **1**–**3** at the B3LYP level are shown in Figure S11 in the SI. Although no symmetry constraints have been applied, the calculated structures for **1**–**3** are symmetrical, adopting the point groups C_s, C_s, and C_i, respectively. Selected calculated and experimental bond lengths and angles for compounds **1**–**3** are given in Table S5 in the SI. An overall agreement has been found between the calculated and experimental geometrical parameters of

dx.doi.org/10.1021/ic301282q | Inorg. Chem. 2012, 51, 13138–13147

compounds **1**–**3**. The metal–ligand bond lengths are always longer than the experimental values particularly at the BP86 level, a fact that has been attributed to interatomic interactions present in the solid state.[23,24]

Cis–Trans Geometrical Isomerism in 2 and 3. The calculated energy difference between compounds **2** and **3**, which exhibit cis–trans geometrical isomerism (Scheme 3), is very small, and the trans isomer **3** is more stable than the cis isomer **2** by 5.8 kcal/mol. Thus, isolation of the cis or trans isomer could be attributed to small differences in the preparation conditions (different pH values). The higher thermodynamic stability of the trans isomer is in agreement with the trans arrangement observed for the structurally characterized dinuclear compounds containing the $\{Mo^{VI}_2O_4\}^{4+}$ moiety.[14a,21] Solvation and hydrogen bonding presumably stabilize at lower pH values the more polar cis isomer than the trans isomer.

Energetics of the Metal Fragment–Ligand Interaction in 1–3. The strength of the overall interaction between the metal fragments *cis*-$[Mo^{VI}O_2]^{2+}$ and *cis*/*trans*-$[Mo_2{}^{VI}O_2(\mu_2\text{-}O_2)(H_2O)_2]^{4+}$ and the ligand dianion ($bihyat^{2-}$) has been calculated for the three molybdenum(VI) compounds. The adiabatic interaction energy (ΔE_{int}, eq 5), between the metal and ligand fragments to get the three $Mo^{VI}bihyat^{2-}$ compounds, has been corrected by taking into account the basis set superposition error, that is

$$\Delta E_{int} = \Delta E + \Delta E_{BSSE} \quad (5)$$

where ΔE gives the uncorrected interaction energy, that is, the difference between the energy of the whole molecule and the sum of energies of its fragments, and ΔE_{BSSE} the basis set superposition error calculated. The calculated values, given in Table 3, reveal that the interaction energies in compounds **2** and **3**, i.e., the cis/trans geometrical isomers, are almost the same.

Table 3. Calculated Metal Fragment (M)–Ligand (L) Interaction Energy for the Complexes Studied[a]

	M	L	ΔE	ΔE_{BSSE}[b]	ΔE_{int}[c]
1	*cis*-$[Mo^{VI}O_2]^{2+}$	$[bihyat]^{2-}$	−813.1	17.2	−796.0
2	*cis*-$[Mo_2{}^{VI}O_2(\mu_2\text{-}O_2)(H_2O)_2]^{4+}$	$[bihyat]_2{}^{4-}$	−1958.3	35.2	−1923.1
3	*trans*-$[Mo_2{}^{VI}O_2(\mu_2\text{-}O_2)(H_2O)_2]^{4+}$	$[bihyat]_2{}^{4-}$	−1960.4	36.1	−1924.3

[a]Energies in kcal/mol. [b]Basis set superposition error. [c]The adiabatic interaction energy, ΔE_{int}, is given by eq 5.

Vibrational Spectra of Compounds 1–3. Calculation of the Hessian for the three molybdenum(VI)-optimized structures gave the frequencies of the fundamental vibrations. The symmetric and asymmetric stretching frequencies of the *cis*-$\{MoO_2\}^{2+}$ group for the mononuclear compound **1** have been calculated as 921 and 927 cm^{-1} with intensities 170 and 210 kM mol^{-1}, respectively, and correspond to the experimental bands at 915 and 948 cm^{-1}, respectively. The calculated frequencies of the normal modes concerning the *cis*- or *trans*-$\{Mo_2{}^{VI}O_2(\mu_2\text{-}O)_2\}^{4+}$ fragment in the dinuclear compounds **2** and **3** along with the experimental values are given in Table 4. In complexes **2** and **3**, the experimental band at about 720 cm^{-1} seems not to be differentiated from cis–trans isomerization and should be assigned to the calculated normal mode located next to $\{Mo(\mu_2\text{-}O)_2Mo\}$ and shown in Figure 9a. On the contrary, the calculated normal modes corresponding to Mo=O-centered vibrations are greatly affected from the cis or trans conformation of the $\{Mo^{VI}O(\mu_2\text{-}O)_2Mo^{VI}O\}^{4+}$ group, as shown in Table 4. In complex **2**, i.e., the cis isomer, the two such normal modes calculated with nonzero intensity are shown in Figure 9b,c. Thus, the two bands at 913 and 947 cm^{-1} are assigned to these two Mo=O-centered vibrations. In the case of complex **3**, i.e., the trans isomer, only one of the calculated normal modes, shown in Figure 9d,e, is IR-active and corresponds to the experimental band at 949 cm^{-1} for **3**. Thus, it seems that the existence of only one well-defined strong band in the 900–950 cm^{-1} region could serve as a diagnostic tool for the trans configuration in related species.

Table 4. Calculated and Experimental Vibrational Frequencies[a] **for Compounds 2 and 3**

2		3	
calcd	exptl	calcd	exptl
$\{Mo(\mu_2\text{-}O_2)Mo\}$ Vibrations[a]			
689 (719)	715s	670 (951)	719s
Mo=O-Centered Vibrations[a]			
918 (38)	914s	884 (0)	
926 (223)	947s	899 (101)	949s
Ligand Vibrations[a]			
1483 (35)	1436m		
1485 (568)	1500m	1481 (285)	1480m
1524 (622)	1542vs,br		
1525 (237)	1565vs,br	1507 (3775)	1540vs
1603 (202)	1651s	1569 (591)	1601s
1612 (189)	1667s	1639 (476)	1668s

[a]The characteristic calculated normal modes, a–f, of compounds **2** and **3** are shown in Figure 9.

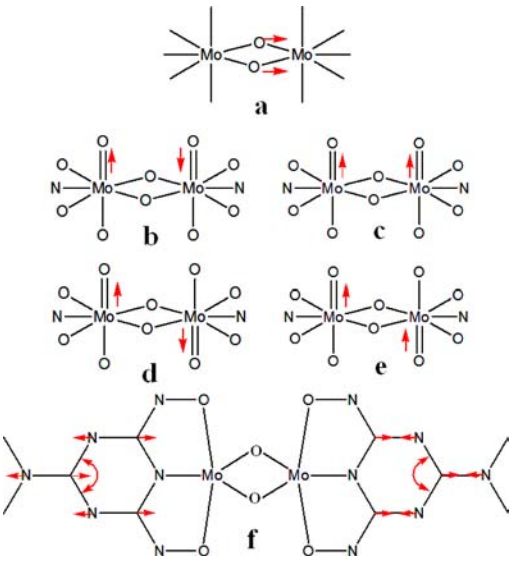

Figure 9. Characteristic calculated normal modes of compounds **2** and **3**.

Detailed analysis of the ligand vibrations of the mononuclear species has already been done.[13a] Thus, the following discussion will be restricted to the differences in the ligand normal modes of the cis and trans dinuclear complexes. The most characteristic ligand calculated and experimental

dx.doi.org/10.1021/ic301282q | Inorg. Chem. 2012, 51, 13138–13147

frequencies are given in Table 4. Again the difference in the spectra of cis and trans complexes comes from the number of triazine ring C−N vibrations. In the trans complexes, there are four such normal modes, giving rise to four sharp bands in the 1500−1650 cm^{-1} region of the experimental spectra of complex **3**. The normal mode corresponding to the most intense band in all compounds, that is, the frequency about 1540 cm^{-1}, is shown in Figure 9f.

Investigation of the Mechanism of the Dimerization Process. In order to evaluate the influence of water on the dimerization of **1** to *cis/trans*-$[Mo_2^{VI}O_2(\mu_2\text{-}O_2)(bihyat)_2(H_2O)_2]$ (**2**/**3**), geometry optimizations and calculations of the thermodynamic parameters of a series of intermediates leading to the dinuclear species **2** and **3** have been carried out. The two possible mechanisms for the transformation of **1** to **2**/**3** along with energy data are depicted in Scheme 6. In the first mechanism, the dimerization process

Scheme 6

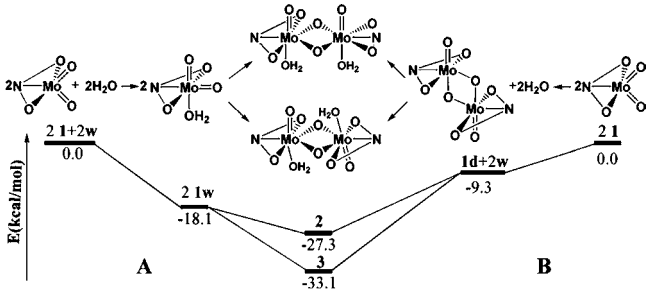

(eq 6 and Scheme 6A) is ideally broken into two steps, the first one being ligation of a water molecule to get the six-coordinate $[Mo^{VI}O_2(bihyat)(H_2O)]$ (**1w**) fragment (eq 7) and the second one being dimerization of the latter (eq 8).

$$2\textit{cis}\text{-}[Mo^{VI}O_2(bihyat)] + 2H_2O \rightarrow \textit{cis/trans}\text{-}[Mo_2^{VI}O_2(\mu_2\text{-}O_2)(bihyat)_2(H_2O)_2] \quad (6)$$

$$\textit{cis}\text{-}[Mo^{VI}O_2(bihyat)] + H_2O \rightarrow \underset{\mathbf{1w}}{[Mo^{VI}O_2(bihyat)(H_2O)]} \quad (7)$$

$$2[Mo^{VI}O_2(bihyat)(H_2O)] \rightarrow \textit{cis/trans}\text{-}[Mo_2^{VI}O_2(\mu_2\text{-}O_2)(bihyat)_2(H_2O)_2] \quad (8)$$

A stabilization energy of 18.1 kcal/mol is calculated for the formation of species **1w**. The optimized structure of **1w** is shown in Figure 10A, and its calculated geometrical parameters are listed in Table S6 in the SI. The molybdenum atom in **1w** has a severely distorted octahedral geometry with a weakly bound water molecule [$d(Mo-O_w)$ = 2.664 Å]. In a final step, compounds **2** (cis dinuclear) and **3** (trans dinuclear) are derived from dimerization of **1w** with a calculated energy gain of 9.1 and 14.9 kcal/mol, respectively.

In the second mechanism (Scheme 6B), two mononuclear molecules of **1** are dimerized first to the dinuclear species $[Mo_2^{VI}O_2(\mu_2\text{-}O_2)(bihyat)_2]$ (**1d**) with a calculated stabilization energy of 9.4 kcal/mol and then ligation of two water molecules to **1d** leads to compounds **2** and **3** with calculated energy gains of 17.9 and 23.7 kcal/mol, respectively. The species **1d** has a highly symmetric (point group C_{2h}) optimized structure and is shown in Figure 10B, and its calculated geometrical parameters

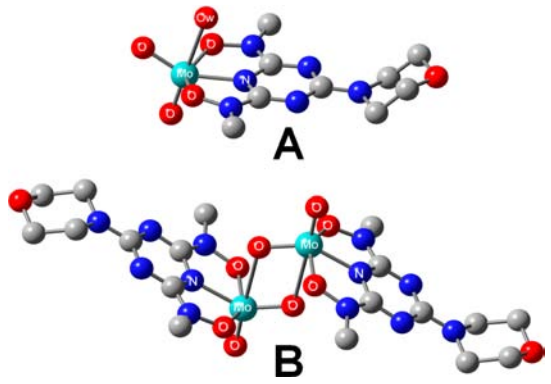

Figure 10. Optimized geometries of the intermediate molybdenum(VI) compounds **1w** (A) and **1d** (B) in the mechanism of dimerization of compound **1**.

are listed in Table S6 in the SI. In the dinuclear compound **1d**, each molybdenum atom has a distorted octahedral coordination environment. The two oxido bridges in **1d** are highly unsymmetrical with short [$d(Mo-O_{b1})$ = 1.764 Å] and very long [$d(Mo-O_{b2})$ = 2.839 Å] bonds, and the two terminal oxido groups are in a trans arrangement, in agreement with the literature data,[14a,21] where the four structurally characterized $\{Mo^{VI}{}_2O_4\}^{4+}$ compounds containing tridentate Schiff bases have the same structural features.

The energy changes for both mechanisms are in favor of the seven-coordinate dinuclear compounds **2** and **3**. Examination of each separate step reveals that the mononuclear six-coordinate adduct **1w** is energetically more favorable, relative to the dinuclear **1d** fragment. Moreover, the addition of water molecules to the six-coordinate molybdenum atoms in **1d** should be more difficult for steric reasons. Thus, it is reasonable to assume that the first mechanism (coordination of water/dimerization) of conversion of **1** to **2**/**3** is more plausible. In marked contrast, in the dimerization process of the six-coordinate mononuclear compounds *cis*-$[Mo^{VI}O_2LD]$[25] (L_2^- = tridentate Schiff base; D = H_2O, CH_3OH, C_2H_5OH, etc.), the first step involves decoordination of D and the second step involves dimerization (Scheme 6B) of the five-coordinate species *cis*-$[Mo^{VI}O_2L]$ to the dinuclear species *trans*-$[Mo^{VI}{}_2O_2(\mu_2\text{-}O_2)L_2]$. Decoordination of the monodentate ligand D in this class of compounds results in an increase of the electrophilicity of the molybdenum atom that attacks one oxido group of the five-coordinate species *cis*-$[Mo^{VI}O_2L]$, and the dimer *trans*-$[Mo^{VI}{}_2O_2(\mu_2\text{-}O_2)L_2]$ is formed.

■ RELATIONSHIP TO BIOLOGICAL SYSTEMS

Our work shows that the electron-donating properties of the Mo^{VI}═O group are strongly dependent on the coordination environment around Mo^{VI}. More specifically, a subtle change in the coordination environment of the five-coordinate compound **1**, with weak ligation of a water molecule (**1w**) trans to an oxido group [$d(Mo-O_{H_2O})$ = 2.664 Å], renders the equatorial oxido group in **1w** more nucleophilic than that in **1**, and this oxido group attacks a molybdenum atom and thus the dinuclear compounds **2**/**3** are formed containing the structural unit $\{O{=}Mo(\mu\text{-}O)_2Mo{=}O\}^{4+}$. The calculated Mulliken charges on the oxygen atoms in compounds **1** and **1w** (Scheme 7) confirm the increased nucleophilicity of the equatorial oxygen atom in **1w**.[26] The nucleophilic attack of the terminal oxygen atom of molybdenum enzymes on substrates is a key step in the

dx.doi.org/10.1021/ic301282q | *Inorg. Chem.* 2012, 51, 13138−13147

Scheme 7

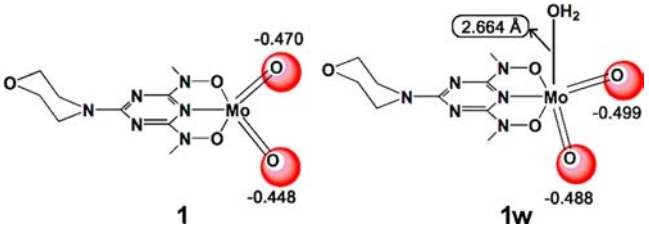

reaction mechanisms of the oxidation of various substrates,[27,28] including the oxidation of sulfite and hypoxanthine by sulfite oxidase and xanthine oxidase, respectively.

CONCLUSIONS

We have synthesized and structurally characterized the mononuclear molybdenum(VI) compound **1** and the dinuclear compounds **2** and **3**. The three compounds represent the first molybdenum complexes with bis(hydroxyamino)-1,3,5-triazine-type ligands, which constitute a class of complexing agents for metal ions in their highest oxidation states (i.e., Ti^{IV} and V^{V}). Compound **1** undergoes a conversion into the dinuclear species **2** and **3** upon ligation of a water molecule. This subtle change in the coordination environment of the five-coordinate compound **1** with ligation of a weakly bound water molecule trans to the oxido ligand (**1w**) renders the equatorial oxido group in **1w** more nucleophilic than that in **1**, and this oxido group attacks a molybdenum atom and thus the dinuclear compounds **2** and **3** are formed. The potentiometric study of the Mo^{VI}bihyat^{2-} system revealed that the Mo^{VI}bihyat^{2-} complexes are hydrolytically stable over a narrow pH range (3−5).

ASSOCIATED CONTENT

Supporting Information

Experimental details for physicochemical measurements, Figures S1−S11, Tables S1−S6, and X-ray crystallographic files in CIF format for the structures of compounds **1**, **2**·8D_2O, and **3**·2D_2O·2CD_3CN. This material is available free of charge via the Internet at http://pubs.acs.org.

AUTHOR INFORMATION

Corresponding Author

*E-mail: (T.V.), (T.K.), (M.P.S.), (A.D.K.), tkampano@cc.uoi.gr (T.A.K.). Tel: (+30)26510-98415. Fax: (+30)26510-98786.

Notes

The authors declare no competing financial interest.

ACKNOWLEDGMENTS

This research is part of the PENED03 research project, implemented within the framework of the "Reinforcement Program of HumanResearch Manpower" (PENED) and cofinanced by National and Community Funds (25% from the Greek Ministry of Development, General Secretariat of Research and Technology, and 75% from EU, European Social Fund). We are also grateful to Dr. Panagiotis Kyritsis for his fruitful comments on the relationship of this piece of work with biological systems. R. Masala is acknowledged for typing this manuscript.

REFERENCES

(1) Compounds **2** (cis dinuclear) and **3** (trans dinuclear) when isolated as amorphous solids contain 0.4 and 1.7 water molecules, respectively, while as crystalline materials, they contain 8 water and 2 water plus 2 acetonitrile molecules, respectively. Throughout the whole paper, these dinuclear species will be reported as **2** and **3** to avoid confusion, except in cases where it is necessary to report the solvents of crystallization.

(2) (a) Zumft, W. G.; Mortenson, L. E. *Biochim. Biophys. Acta* **1975**, *416*, 1−52. (b) Burgess, B. K. *Chem. Rev.* **1990**, *90*, 1377−1406. (c) Kirn, J.; Rees, D. C. *Nature* **1992**, *360*, 553−560.

(3) (a) Tenderholt, A. L.; Wang, J.-J.; Szilagyi, R. K.; Holm, R. H.; Hodgson, K. O.; Hedman, B.; Solomon, E. I. *J. Am. Chem. Soc.* **2010**, *132*, 8359−8371. (b) Hille, R. *Chem. Rev.* **1996**, *96*, 2757−2816. (c) Hille, R. *Trends Biochem. Sci.* **2002**, *27*, 360−367. (d) Romao, M. *Dalton Trans.* **2009**, 4053−4068. (e) Pushie, M. J.; Doonan, C. J.; Moquin, K.; Weiner, J. H.; Rothery, R.; George, G. N. *Inorg. Chem.* **2011**, *50*, 732−740.

(4) (a) Volpe, M.; Mosch-Zanetti, N. C. *Inorg. Chem.* **2012**, *51*, 1440−1449. (b) Arumuganathan, T.; Volpe, M.; Harum, B.; Wurm, D.; Belaj, F.; Mosch-Zanetti, N. C. *Inorg. Chem.* **2012**, *51*, 150−156.

(5) (a) Mitchell, J. M.; Finney, N. S. *J. Am. Chem. Soc.* **2001**, *123*, 862−869 and references cited therein. (b) Gamelas, C. A.; Gomes, A. C.; Bruno, S. M.; Almeida Paz, F. A.; Valente, A. A.; Pillinger, M.; Romãoa, C. C.; Gonçalves, I. S. *Dalton Trans.* **2012**, 00.

(6) (a) Neves, P.; Gago, S.; Balula, S. S.; Lopes, A. D.; Valente, A. A.; Cunha-Silva, L.; Almeida Paz, F. A.; Pillinger, M.; Rocha, J.; Silva, C. M.; Gonçalves, I. S. *Inorg. Chem.* **2011**, *50*, 3490−3500. (b) Coelho, A. C.; Nolasco, M.; Balula, S. S.; Antunes, M. M.; Pereira, C. C. L.; Almeida Paz, F. A.; Valente, A. A.; Pillinger, M.; Ribeiro-Claro, P.; Klinowski, J.; Gonçalves, I. S. *Inorg. Chem.* **2011**, *50*, 525−538.

(7) (a) Brewer, P. G. In *Chemical Oceanography*, 2nd ed.; Riley, J. P., Skirrow, G., Eds.; Academic Press: New York, 1975; Vol. *1*, pp 415−496. (b) Mohamed, M. A.; Kataoka, M.; Ohzeki, K. *Analyst* **1985**, *110*, 125.

(8) (a) *Bioinorganic Vanadium Chemistry*; Rehder, D., Ed.; John Wiley & Sons Ltd.: West Sussex, England, 2008. (b) Garner, C. D.; Armstrong, E. M.; Berry, R. E.; Beddoes, R. L.; Collison, D.; Cooney, J. J. A.; Ertok, S. N.; Helliwell, M. J. *Inorg. Biochem.* **2000**, *80*, 17−20. (c) Armstrong, E. M.; Beddoes, R. L.; Calviou, L. J.; Charnock, J. M.; Collison, D.; Ertok, N.; Naismith, J. H.; Garner, C. D. *J. Am. Chem. Soc.* **1993**, *115*, 807−808.

(9) (a) Armstrong, E. M.; Collison, D.; Ertok, N.; Garner, C. D. *Talanta* **2000**, *53*, 75−87. (b) Berry, R. E.; Armstrong, E. M.; Beddoes, R. L.; Collison, D.; Ertok, S. N.; Helliwell, M.; Garner, C. D. *Angew. Chem., Int. Ed.* **1999**, *38*, 795−797. (c) Smith, P. D.; Berry, R. E.; Harben, S. M.; Beddoes, R. L.; Helliwell, M.; Collison, D.; Garner, C. D. *J. Chem. Soc., Dalton. Trans.* **1997**, *23*, 4509−4516.

(10) Bayer, E.; Koch, E.; Anderegg, G. *Angew. Chem., Int. Ed. Engl.* **1987**, *26*, 545−546.

(11) (a) Smith, P. D.; Cooney, J. J. A.; McInnes, E. J. L.; Beddoes, R. L.; Collison, D.; Harben, S. M.; Helliwell, M.; Mabbs, F. E.; Mandel, A.; Powell, A. K.; Garner, C. D. *Dalton. Trans.* **2001**, 3108−3114. (b) Harben, S. M.; Smith, P. D.; Beddoes, R. L.; Collison, D.; Garner, C. D. *J. Chem. Soc. Dalton. Trans.* **1997**, 2777−2784. (c) Yadav, H. S.; Armstrong, E. M.; Beddoes, R. L.; Collison, D.; Garner, C. D. *J. Chem. Soc., Chem. Commun.* **1994**, 605−606.

(12) (a) Gun, J.; Ekeltchik, I.; Lev, O.; Shelkov, R.; Melman, A. *Chem. Commun.* **2005**, 5319−5321. (b) Ekeltchik, I.; Gun, J.; Lev, O.; Shelkov, R.; Melman, A. *Dalton Trans.* **2006**, 1285−1293. (c) Peri, D.; Alexander, J. S.; Tshuva, E. Y.; Melman, A. *Dalton Trans.* **2006**, 4169−4172. (d) Shavit, M.; Peri, D.; Melman, A.; Tshuva, E. Y. *J. Biol. Inorg. Chem.* **2007**, *12*, 825−830. (e) Hermon, T.; Tshuva, E. Y. *J. Org. Chem.* **2008**, *73*, 5953−5958. (f) Melman, G.; Vimal, P.; Melman, A. *Inorg. Chem.* **2009**, *48*, 8662−8664. (g) Bou-Abdallah, F.; McNally, J.; Liu, X. X.; Melman, A. *Chem. Commun.* **2011**, 731−733.

(13) (a) Nikolakis, V. A.; Tsalavoutis, J. T.; Stylianou, M.; Evgeniou, E.; Jakusch, T.; Melman, A.; Sigalas, M. P.; Kiss, T.; Keramidas, A. D.; Kabanos, T. A. *Inorg. Chem.* **2008**, *47*, 11698−11710. (b) Nikolakis, V.

A.; Exarchou, V.; Jakusch, T.; Woolins, J. D.; Slawin, A. M. Z.; Kiss, T.; Kabanos, T. A. *Dalton Trans.* **2010**, *39*, 9032−9038.
(14) (a) Wieghardt, K.; Holzbach, W.; Weiss, J. *Inorg. Chem.* **1981**, *20*, 3436−3439. (b) Crans, D. C.; Smee, J. J.; Gaidamauskiene, E. G.; Anderson, O. P.; Miller, S. M.; Jin, W. Z.; Gaidamauskas, E.; Crubellier, E.; Grainda, R.; Chi, L. H.; Willsky, G. R. *J. Inorg. Biochem.* **2004**, *98*, 1837−1850.
(15) (a) Smee, J. J.; Epps, J. A.; Teissedre, G.; Maes, M.; Harding, N.; Yang, L.; Baruah, B.; Miller, S. M.; Anderson, O. P.; Willsky, G. R.; Crans, D. C. *Inorg. Chem.* **2007**, *46*, 9827−9840. (b) Ooms, K. J.; Bolte, S. E.; Smee, J. J.; Baruah, B.; Crans, D. C.; Polenova, T. *Inorg. Chem.* **2007**, *46*, 9285−9293. (c) Keramidas, A. D.; Miller, S. M.; Anderson, O. P.; Crans, D. C. *J. Am. Chem. Soc.* **1997**, *119*, 8901. (d) Paul, P. C.; Angus-Dunne, S. J.; Batchelor, R. J.; Einstein, F. W. B.; Tracey, A. S. *Can. J. Chem.* **1997**, *75*, 429−440. (e) Wieghardt, K.; Quilitzsch, U.; Nuber, B.; Weiss, J. *Angew. Chem., Int. Ed. Engl.* **1978**, *17*, 351−352.
(16) Nikolakis, V. A.; Stathopoulos, P.; Exarchou, V.; Gallos, J. K.; Kubicki, M.; Kabanos, T. A. *Inorg. Chem.* **2010**, *49*, 52−61.
(17) Belock, C. W.; Cetin, A.; Barone, N. V.; Ziegler, C. J. *Inorg. Chem.* **2008**, *47*, 7114−7120.
(18) Upon the addition of H_2bihyat, the pH of the $Na_2Mo^{VI}O_4{\cdot}2H_2O$ aqueous solution (pH 3.5) was raised (see eq 2), and its final value, after 12 h of stirring, was ∼5.5.
(19) $Mo^{V}Cl_5$ (0.100 g) was dissolved in water (5 mL), the pH of the solution (∼0.0) was adjusted to ∼3.5 with an aqueous sodium hydroxide solution (2 M), and then solid H_2bihyat in an equivalent quantity was added in one portion to the above stirred solution. The pH of the reaction mixture was kept at pH ∼3.5 with 2 M HCl. After an additional 12 h of stirring, compound **2** (see eq 3) was isolated.
(20) A τ value of 1 corresponds to an ideal trigonal-bipyramidal geometry, and a τ value of 0 corresponds to an ideal square-pyramidal geometry. See: Addison, A. W.; Rao, T. N.; Reedjik, J.; van Rijn, J.; Verschoor, G. C. *J. Chem. Soc., Dalton Trans.* **1984**, 1349−1356.
(21) (a) Sobczak, J. M.; Glowiak, T.; Ziokowski, J. J. *Transition Met. Chem.* **1990**, *15*, 208−211. (b) Mo, S. J.; Koo, B. K. *Bull. Korean Chem. Soc.* **1999**, *20*, 1105. (c) Lehtonen, A.; Sillanpää, R. *Polyhedron* **2005**, *24*, 257−265. (d) Cindrić, M.; Vrdoljak, V.; Strukan, N.; Kamenar, B. *Polyhedron* **2005**, *24*, 369−376.
(22) (a) Manos, M. J.; Keramidas, A. D.; Woollins, J. D.; Slawin, A. M. Z.; Kabanos, T. A. *J. Chem. Soc., Dalton Trans.* **2001**, 3419−3420. (b) Manos, M. J.; Woollins, J. D.; Slawin, A. M. Z.; Kabanos, T. A. *Angew. Chem., Int. Ed.* **2002**, *41*, 2801−2805. (c) Modec, B.; Brencic, J. V.; Koller, J. *Eur. J. Inorg. Chem.* **2004**, 1611−1620. (d) Modec, B.; Brencic, J. V. *Eur. J. Inorg. Chem.* **2005**, 4325−4334. (e) Modec, B.; Dolenc, D.; Brencic, J. V.; Koller, J.; Zubieta, J. *Eur. J. Inorg. Chem.* **2005**, 3224−3237. (f) Modec, B.; Dolenc, D.; Kasunic, M. *Inorg. Chem.* **2008**, *47*, 3625−3633. (g) Modec, B.; Sala, M.; Clérac, R. *Eur. J. Inorg. Chem.* **2010**, 542−553.
(23) Jonas, V.; Frenking, G.; Reetz, M. T. *J. Am. Chem. Soc.* **1994**, *116*, 8741.
(24) Bray, M. R.; Deeth, R. J.; Paget, V. J.; Sheen, P. D. *Int. J. Quantum Chem.* **1996**, *61*, 85.
(25) (a) Sobczak, J. M.; Glowiak, T.; Ziolkowski, J. J. *Transition Met. Chem.* **1990**, *15*, 208−211. (b) Rajan, O. A.; Chakravorty, A. *Inorg. Chem.* **1981**, *20*, 660−664. (c) Cindric, M.; Strukan, N.; Vrdoljak, V.; Kajfez, T.; Kamenar, B. *Z. Anorg. Allg. Chem.* **2002**, *628*, 2113−2117. (d) Lal, R. A.; Basumatary, D.; Adhikari, S.; Kumar, A. *Spectrochim. Acta, Part A* **2008**, *69*, 706−714. (e) Agustin, D.; Bibal, C.; Neveux, B.; Daran, J.-C.; Poli, R. *Z. Anorg. Allg. Chem.* **2009**, *635*, 2120−2125.
(26) The calculated Mulliken charge of the axial oxido ligand in **1w** is also increased but to a lesser extent in comparison to its equatorial oxido ligand.
(27) (a) Doonan, C. J.; Stockert, A.; Hille, R.; George, G. N. *J. Am. Chem. Soc.* **2005**, *127*, 4518−4522. (b) Fu, G.; Xu, X.; Lu, X; Wan, H. *J. Phys. Chem. B* **2005**, *109*, 6416−6421. (c) Yin, G. *Coord. Chem. Rev.* **2010**, *254*, 1826−1842.
(28) (a) Bonin, I.; Martins, B. M.; Purvanov, V.; Fetzner, S.; Huber, R.; Dobbek, H. *Structure* **2004**, *12*, 1425−1435. (b) Okamoto, K.; Matsumoto, K.; Hille, R.; Eger, B. T.; Pai, E. F.; Nishino, T. *Proc. Natl. Acad. Sci. U.S.A.* **2004**, *101*, 7931−7936.